Wide-Range Position-Tuning Lasers in Cholesteric Liquid Crystal

2013 Chinese Phys. Lett. 30 084206

(http://iopscience.iop.org/0256-307X/30/8/084206)

CHIN. PHYS. LETT. Vol. 30, No. 8 (2013) 084206

Wide-Range Position-Tuning Lasers in Cholesteric Liquid Crystal *

DAI Qin(岱钦)[1], LI Yong(李勇)[1], WU Jie(吴杰)[1], ZHANG Meng(张濛)[1], WU Ri-Na(乌日娜)[1**], PENG Zeng-Hui(彭增辉)[2], YAO Li-Shuang(姚丽双)[2]

[1]*School of Science, Shenyang Ligong University, Shenyang 110159*
[2]*State Key Laboratory of Applied Optics, Changchun Institute of Optics, Fine Mechanics and Physics, Chinese Academy of Sciences, Changchun 130033*

(Received 20 May 2013)

A wedge liquid crystal (LC) cell is designed and manufactured, and a dye-doping cholesteric LC laser formed by mutual diffusion of the cholesteric LC with different pitches. A laser that is tunable in the 558–624 nm range is obtained under moderate optical pumping, with a tuning range of 66 nm and a laser spectral tuning resolution of 1 nm, so as to achieve the spatial position of a wide range of tunable lasers. The laser threshold varies at different positions in the device, and the lasing thresholds of the dye-doping cholesteric LC cell at 40 and 9 μm are 18 and 25 μJ/pulse, respectively. The density of the photonic states is simulated in the experimental sample, and the result is in good agreement with the photonic band gap in our experiment, which not only explains the low-threshold laser at the band gap edge, but also predicts the experiment.

PACS: 42.55.Tv, 42.79.Kr, 42.70.Hj DOI: 10.1088/0256-307X/30/8/084206

The lasing properties of cholesteric liquid crystals (CLCs) have attracted considerable attention.[1−14] Laser dye is doped in a planar arrangement in cholesteric liquid crystal (LC) devices. According to Fermi's golden rule, the rate of spontaneous emission is proportional to the density of the photonic states in the media, which promotes the appearance of laser emission near the selective reflection band edge. A sharply enhanced density of states at the band-edge of the photonic band gap (PBG) leads to a low-threshold lasing operation near the band-edge for moderate optical pumping.[1−4] The PBG has a central wavelength $\lambda = np$, and helical pitch $p = 1/(c \cdot P_{\mathrm{HTP}})$, where n is the average refractive index, P_{HTP} is the helical twisting power, and c is the concentration of the chiral agent. The pitch p is very sensitive to its environment, such as the temperature, mechanical stress, electric, magnetic and acoustic fields.[5,6] Thus a tunable laser could be achieved under different external field conditions. The photonic crystal tunable laser based on LCs has wide applications in optical displays, optical communication, photonic integration and biomedical engineering, etc, because of its simple production process, less optical loss, low-threshold and small volume.[4,7,8] However, a large number of investigations show that tunable LC lasers are controlled by an electric field and temperature.[7]

If a spatial pitch gradient is formed in a dye-doping CLC cell, the output laser wavelength can be tuned. A spatial pitch gradient is built-in by various means, such as a thermal gradient control in a fixed chiral dopant concentration, a position control of UV curing, and diffusion between two chiral dopant concentrations.[8−13] In this Letter, in order to achieve a wide-range tunable wavelength, CLCs with two kinds of dye-doping concentrations are injected into a wedge cell. The wedge cell provides discontinuous pitch jumps, which can easily be tunable for CLC lasers.

An ITO glass substrate was coated by a polyimide orientation film, and the wedge cells were fabricated using spacers at two different sizes of 9 μm and 40 μm, and then sealed and solidified. Their structure is shown in Fig. 1. Two kinds of dye-doped CLCs were produced, one is composed of a nematic LC (TEB30A), chiral agent (S811), and laser dye (PM580), and their concentrations are 69%, 29%, 2%, respectively. The other is composed of nematic LC (TEB30A), chiral agent (S811), and dye (DCM), with concentrations of 72.4%, 25.6%, 2%. Two kinds of dye-doped CLCs were mixed by a magnetic stirrer. In order to mix them thoroughly, the mixing time was more than nine hours. They were then injected into the cell by half-filling. Finally, the CLC wedge cells were kept at room temperature for more than two weeks to develop a pitch gradient through diffusion of the helical rotatory power.

Due to the formed pitch gradient in this device, different colors were seen at different positions of the cell under white light, as shown Fig. 2(a). The obvious planar texture was observed by an orthogonal polarization microscope. This phenomenon indicates that

*Supported by the National Natural Science Foundation of China under Grant No 60777011, the Natural Science Foundation of Liaoning Province under Grant No L2010465, and Technology Project of Education Department of Liaoning Province under Grant No L2012070.

**Corresponding author. Email: wurina2007@126.com

it has a screw period arrangement, with the helix axis perpendicular to the glass substrate, and minor color changes are observed in different shooting positions, as shown in Fig. 2(b).

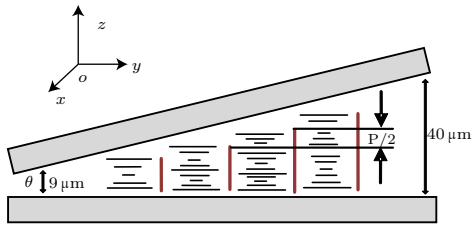

Fig. 1. Schematic diagram of the wedge cell.

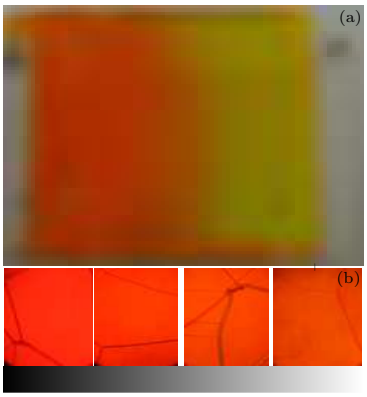

Fig. 2. (a) Photographic image of the wedge cell, and (b) polarized microscope images at different spatial positions.

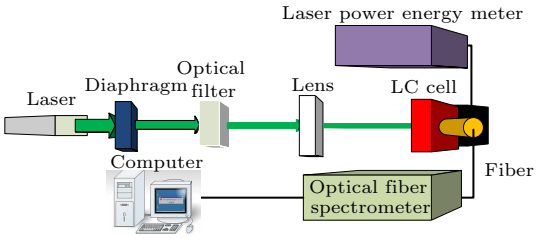

Fig. 3. The measurement device of the laser radiation spectrum.

The experimental device is shown in Fig. 3. A second-harmonic Q-switched Nd:YAG laser at $\lambda = 532\,\text{nm}$ was employed to pump the dye-doped CLC sample. Its pulse width and repetition rate were 20 ns and 5 Hz, respectively. The pump beam was focused by a lens and its waist at the focal point was 500 μm. The angle was 45° between the pumping beam and the normal line of the sample surface. A laser radiation spectrum was measured by the optical fiber probe of the spectrometer (Avantes), which is perpendicular to the glass substrate.

The transmitted and laser radiation spectra were measured at different positions of the cell, as shown in Fig. 4. The transmitted spectrum was vertically measured by a UV spectrophotometer (UV757CRT), as shown in Fig. 4(a). The photonic band gap movements can be clearly observed in the figure. The photonic band gap edge changes when incident light irradiates at different locations. The long wave edge was detected with measurement locations with LC cells at thicknesses of 2, 4, 6, 8, 10, and 12 mm, and they are 648, 639, 624, 614, 606, and 594 nm, respectively, with a movement of 54 nm. Based on the characteristics of the photonic band gap in the planar arrangement states of CLCs, the long wavelength band edge of the stop band is $\lambda = n_e p$, $n_e = 1.692$ (TEB30A), so the pitches were 382, 377, 368, 362, 358, and 351 nm, respectively, and then the stimulation emission wavelengths were 622, 605, 591, 582, 573, and 561 nm, respectively. This phenomenon indicates that it has a position dependent pitch gradient. There is a mismatch between the laser emission wavelength and the edge of the photonic band-gap long wave because of the angle between the pumping beam and the helix axis.[14] The relation between the central wavelength of the stop band (λ) as a function of θ can be described as $\lambda = np\cos\theta$.[15] The photonic band gap has a blueshift when changing incident angles, which affects the laser output location.

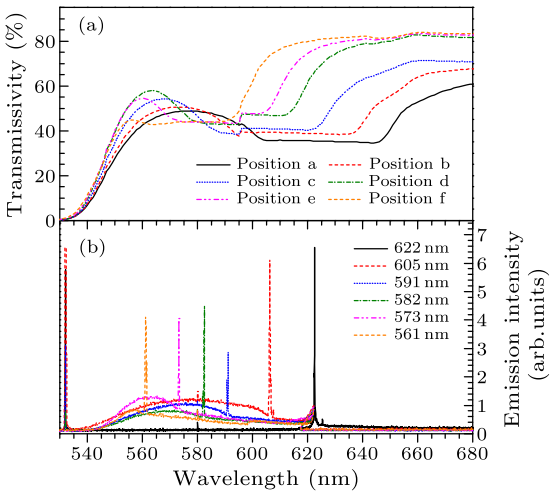

Fig. 4. (a) The transmission spectrum measured by a UV spectrophotometer (UV757CRT) at different positions. (b) Corresponding to the (a) position of the laser radiation spectrum.

For an angle of 45° between the incident light and the normal of the sample surface, as the focused pumping beam scans continuously across the wedge cell from the thick to thin part, the output laser spectrum was measured, as shown in Fig. 5. It can be seen that the stimulated emission wavelength has a minimal change in the range 0–3 mm, which indicates that the concentration gradient is not obvious, and cannot be formed in the region due to the long size of the box. However, according to a property of the wedge cell, surface anchoring is dominant compared with bulk torque, resulting in pitch elongation, and subsequently it has a minimal change in lasing wavelength in this region. However, in the range from

3 to 13 mm, not only pitch elongation but also concentration gradient were formed. Thus, a wide-range wavelength tunable laser was achieved over a range of 56 nm, from 558 nm to 614 nm, with an accuracy of 1 nm in this region.

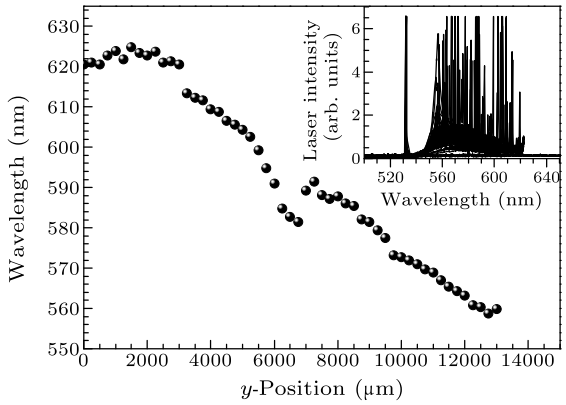

Fig. 5. The laser line as a function of spatial position, with the inset the laser line spectrum.

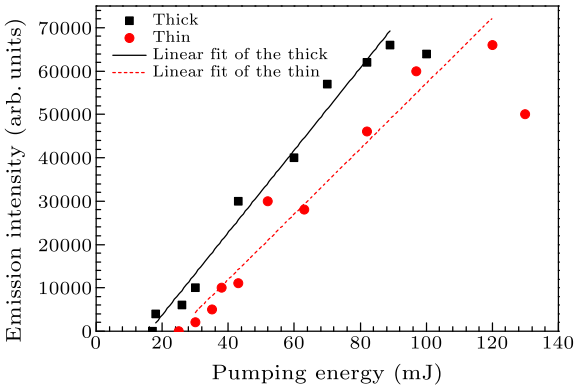

Fig. 6. The laser emission intensity as a function of pumping energy at different locations.

Nevertheless, three discontinuous laser peaks arose in the range 6.2–6.7 mm. There are three possible reasons for this, as follows. (1) Two of the mixed dye-doping CLCs are not uniform, which leads to abnormal laser emittance. (2) The alignment film of the LC glass substrate is not flat, and the geometry gradient in the wedge cell may not be continuous. (3) In order to satisfy the geometry gradient in the wedge cell, the pitch is elongated. However, due to the boundary condition effect, this will be a sudden transition when the two adjacent pitches extend to $P/2$ (P is the screw pitch). In this experiment, the measurement position just falls on it. Further reducing the spot size of the pump source will increase the tuning accuracy. At the same time, the hopping phenomenon in every position of the pitch extending to $P/2$ will be detectable. Figure 6 shows the laser emission intensity as a function of pumping energy in the dye-doping CLC cell. Due to different doping concentrations and cell gaps in different positions, the laser thresholds were 25 μJ, 18 μJ at the thinnest (about 9 μm) and the thickest (about 40 μm) positions in the cell, respectively.

Finally, the CLC laser was prepared. According to the device parameters, the density of photonic states (DOS) was simulated in the experimental sample. The tuning characteristics of the output laser wavelength and the threshold characteristics were measured and analyzed. The effect of the pitch change in the cell on the output laser wavelength tuning characteristics was investigated and discussed.

The curve distribution of the DOS was simulated in this sample based on Blinov's simulation for a transparent plate and a transparent CLC.[16] The DOS is inversed in a group velocity and defined as the density of wavevectors per unit volume and unit angular frequency, and can be deduced from the transmission coefficient of the CLC.[16–18] In order to find the DOS for the dye-doped CLC laser, the light absorption was ignored in the CLC layers and we can write the transmission coefficient of the CLC[17] as

$$t = \frac{4\pi\beta e^{i2\pi L/p}}{4\pi\beta\cos(\beta L) + ip(\beta^2 - k^2 + (2\pi/p)^2)\sin(\beta L)}, \quad (1)$$

where L is the CLC cell thickness, and p is the helical pitch of the CLC. $\pm\beta$ are the wavevectors of the two circularly polarized eigenwaves, which suffer Bragg diffraction upon propagation in two opposite directions along the helical axis and satisfy

$$\beta^2 = k^2 + \left(\frac{2\pi}{p}\right)^2 - k\sqrt{\frac{16\pi^2}{p^2} + k^2\delta^2}. \quad (2)$$

Here, $k^2 = (\omega/c_0)^2\langle\varepsilon\rangle$, with c_0 being the ray velocity and ω the angular frequency; $\langle\varepsilon\rangle = (\varepsilon_{||} + \varepsilon_{\perp})/2$ is the average dielectric permittivity; and δ is the anisotropy, $\delta = (\varepsilon_{||} - \varepsilon_{\perp})/(\varepsilon_{||} + \varepsilon_{\perp})$. The real part ($X$) and the imaginary part (Y) of the transmission of CLC are expressed as[17]

$$X = \frac{16\pi^2\beta^2\cos(\beta L)}{16\pi^2\beta^2 + k^4\delta^2p^2\sin^2(\beta L)}, \quad (3)$$

$$Y = \frac{4\pi\beta(\beta^2p^2 - k^2p^2 + 4\pi^2)\sin(\beta L)}{16\pi^2\beta^2p + k^4\delta^2p^3\sin^2(\beta L)}. \quad (4)$$

Thus, for the calculation of DOS, we only need to calculate the complex transmission coefficient $t = X + iY$. Since the total phase (φ) accumulated by the light wave during propagation through the whole sample is $\varphi = kL$ and $\tan\varphi = Y(\omega)/X(\omega)$, the DOS is deduced as[17,18]

$$\rho(\omega) = \frac{d\varphi(\omega)}{Ld\omega} = \frac{1}{L}\frac{Y'X - X'Y}{X^2 + Y^2}. \quad (5)$$

In this device, the cell thickness and pitch are changed in different positions. According to the sample's parameters (cell thickness and helical pitch), the DOS is

simulated. The distribution of the DOS is shown in Fig. 7(b), and the curve distribution is in good agreement with the PBG in our experiment (Fig. 7(a)), which not only explains the edge of the forbidden band low-threshold laser, but also predicts the experiment.

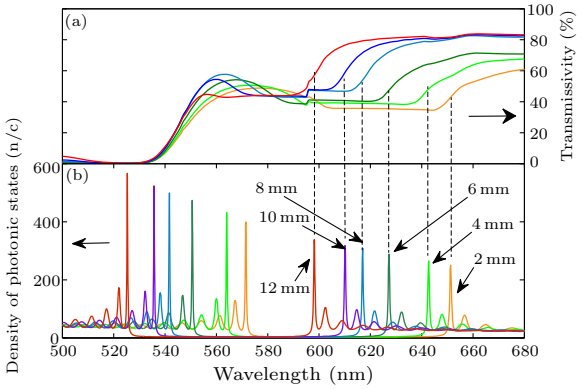

Fig. 7. (a) The transmission spectrum of the experiment. (b) The distribution of the density of photonic states (DOS) at different positions (the arrows denote the different positions in the device).

In summary, a pitch gradient of the dye-doping CLC wedge cell is designed and manufactured. Based on this, a wide range of tunable LC lasers are obtained. Two kinds of dye-doping CLCs are injected into a wedge cell by the half-filled method, and then the PBG characteristics and the spatial position of the output laser tuning properties are measured and analyzed at different positions of the device. The tunable laser at wavelengths from 558 nm to 624 nm is obtained under 532 nm Q-switched laser pumping. The tuning range is 66 nm. Finally, the laser thresholds of the device are measured, different thresholds are obtained at different locations, and the maximum laser threshold is 25 μJ. The DOS is simulated for the device, and the agreement between the simulations and the experimental results not only explains the edge of the forbidden band low-threshold laser, but also predicts the experiment.

References

[1] Kopp V I, Zhang Z Q and Genack A Z 2003 *Prog. Quantum Electron.* **27** 369
[2] Schmidtke J and Stille W 2003 *Eur. Phys. J.* B **31** 179
[3] Ozaki M, Matsuhisa Y, Yoshida H, Ozaki R and Fujii A 2007 *Phys. Status Solidi* **204** 3777
[4] Ford A D, Morris S M and Coles H J 2006 *Mater. Today* **9** 36
[5] Li W C, Zheng Z G, Liu Y G et al 2010 *Opt. Precis. Eng.* **18** 1504
[6] Zhang Y and Zhao H B 2009 *Opt. Precis. Eng.* **17** 1798
[7] Ozaki R, Matsui T et al 2003 *Appl. Phys. Lett.* **82** 3593
[8] Huang Y H, Zhou Y and Wu S T 2006 *Appl. Phys. Lett.* **88** 011107
[9] Chanishvili A, Chilaya G, Petriashvili G, Barberi R, Bartolino R, Cipparrone G, Mazzulla A, Gimenez R, Oriol L and Pinol M 2005 *Appl. Phys. Lett.* **86** 051107
[10] Sonoyama N, Takanishi Y, Ishikawa K and Takezoe H 2007 *J. Appl. Phys.* **46** 874
[11] Furumi S, Yokoyama S, Otomo A and Mashiko S 2004 *Appl. Phys. Lett.* **84** 2491
[12] Chanishvili A, Chilaya G, Petriashvili G, Barberi R, Bartolino R et al 2004 *Adv. Mater.* **16** 791
[13] Jeong M Y, Wu J W 2010 *Opt. Express* **18** 24221
[14] Eidel'man E D 1999 *Phys. Solid State* **41** 148
[15] Dai Q, Wu R N et al 2011 *Opt. Precis. Eng.* **50** 013601
[16] Blinov L M 2009 *JETP Lett.* **90** 166
[17] Belyakov V A 2008 *Ferroelectrics* **364** 33
[18] Bendickson J M, Dowling J P and Scalora M 1996 *Phys. Rev.* E **53** 4107